THE ASTROPHYSICAL JOURNAL, 439:849–853, 1995 February 1

X-RAY SPECTRA FROM NEUTRON STARS ACCRETING AT LOW RATES

LUCA ZAMPIERI,[1] ROBERTO TUROLLA,[2] SILVIA ZANE,[1] AND ALDO TREVES[1]
Received 1994 June 11; accepted 1994 August 3

ABSTRACT

The spectral properties of X-ray radiation produced in a static atmosphere around a neutron star accreting at very low rates are investigated. Previous results by Alme & Wilson are extended to the range $10^{-7} \leq L/L_{\rm Edd} \leq 10^{-3}$ to include the typical luminosities, $L \sim 10^{31}$–10^{32} ergs s^{-1}, expected from isolated neutron stars accreting the interstellar medium. The emergent spectra show an overall hardening with respect to the blackbody at the neutron star effective temperature in addition to a significant excess over the Wien tail. The relevance of present results in connection with the observability of low-luminosity X-ray sources is briefly discussed.

Subject headings: accretion, accretion disks — radiation mechanisms: nonthermal — stars: neutron — X-rays: stars

1. INTRODUCTION

Since the early 1970s large theoretical efforts have been devoted to investigate the properties of radiation produced by accretion onto neutron stars, in the attempt to model the observed spectra of Galactic X-ray sources. Up to now, the interest mainly focused on emergent spectra for luminosities in the range $\sim 10^{35}$–10^{38} ergs s^{-1}, since most of observed X-ray binaries have $L \gtrsim 10^{34}$ ergs s^{-1}. Much fainter sources may, nevertheless, exist. It was suggested long ago (Ostriker, Rees, & Silk 1970), in fact, that old isolated neutron stars (ONSs) no longer active as pulsars, may show up as very weak, soft X-ray sources ($L \sim 10^{31}$–10^{32} ergs s^{-1}) if they accrete the interstellar medium. The capabilities of present instrumentation on board X-ray satellites like *ROSAT*, make now possible the observation of such low-luminosity sources (e.g., Treves & Colpi 1991; Blaes & Madau 1993).

ONSs may have low magnetic fields in which case they would accrete spherically. Spherical accretion onto an unmagnetized neutron star was first considered by Zel'dovich & Shakura (1969, hereafter ZS) and, in more detail, by Alme & Wilson (1973, hereafter AW), who concentrated, however, on high-luminosity solutions. The lack of results for $L \lesssim 10^{-3} L_{\rm Edd}$ led us to reconsider the problem. We compute the spectrum emerging from a static spherical atmosphere surrounding an accreting neutron star in the case of very low rates, extending previous calculations by AW to $L \sim 10^{-7} L_{\rm Edd}$. We found that the resulting spectral distributions are significantly harder than a blackbody at the star effective temperature. Our results may lead us to reconsider the present estimates of the observability of ONSs, which were based on the assumption of a Planckian spectrum.

2. THE MODEL

We consider a nonrotating, unmagnetized neutron star which undergoes spherical accretion and is surrounded by a spherical, static atmosphere; the envelope material is assumed to be pure hydrogen. As the accretion flow penetrates into the atmosphere, protons are decelerated by Coulomb collisions and/or plasma interactions, their bulk kinetic energy is transferred to electrons, and is finally converted into electromagnetic radiation via free-free emission. The input physics of our model essentially coincides with that used in previous studies on this subject. Equilibrium solutions were firstly provided by ZS for the frequency-integrated case, and by AW for the complete transfer problem. These investigations concentrated on the study of high-luminosity regimes ($L \gtrsim 10^{36}$ s^{-1}) and revealed the fundamental role played by Comptonization of primary bremsstrahlung photons in establishing the thermal balance of the emitting gas and the properties of the emerging radiation. The possible existence of a new "hot" solution, in which Comptonization is dominant, was recently discussed by Turolla et al. (1994, Paper I). A detailed modeling of the interactions between the impinging flow and the static envelope is exceedingly complicated (see, e.g., Bildsten, Shapiro, & Wasserman 1992), also because a collisionless, standing shock can form, as originally suggested by Shapiro & Salpeter (1973). Following both ZS and AW (see also Paper I), we circumvent this problem assuming that the proton stopping length is a free parameter of our model, together with the total luminosity L_∞, measured by an observer at infinity. Denoting by ϱ the gas density, the column density of the atmospheric material is $y = \int_R^\infty \varrho \, dR$; the value y_0 corresponding to the proton stopping length was estimated by ZS to be in the range $5 \lesssim y_0 \lesssim 30$ g cm^{-2} when Coulomb collisions are dominant. As it was shown in Paper I, no significant expansion occurs in both "cold" and "hot" envelopes, so we treat the radial coordinate as a constant, equal to the neutron star radius R_*. The heat injected per unit time and mass in the envelope is calculated using the expression for the energy-loss rate due to Coulomb collisions of superthermal protons (see Bildsten et al. 1992),

$$W_h = \begin{cases} \dfrac{L_\infty}{8\pi R_*^2 \, y_0 \, y_G} \dfrac{1 + v_{\rm th}^2/v_i^2}{[1 - (1 - v_{\rm th}^4/v_i^4)(y/y_0)]^{1/2}} & y \leq y_0 \\ 0 \, , & y > y_0 \end{cases} \tag{1}$$

[1] International School for Advanced Studies, Trieste, Via Beirut 2-4, 34014 Trieste, Italy.
[2] Department of Physics, University of Padova, Via Marzolo 8, 35131 Padova, Italy.

where $v_i^2 = c^2(1 - L_\infty/L_{\rm Edd})/3$ is the "modified" free-fall velocity, $v_{\rm th}^2 = 3kT/m_p$ is the proton thermal velocity, $y_G = (1 - 2GM_*/c^2R_*)^{1/2}$ is the gravitational redshift factor in the Schwarzschild spacetime and M_* is the star mass. We note that, owing to the gravitational redshift, the total luminosity seen by a distant observer, L_∞, is related to the local luminosity at the top of the atmosphere by $L_\infty = y_G^2 L(0)$.

The run of pressure P, temperature T, monochromatic radiation energy density U_ν and flux F_ν (both measured by the local observer) are obtained solving the hydrostatic and the energy balance for a completely ionized, perfect hydrogen gas (ZS; Paper I) coupled to the first two frequency-dependent transfer moment equations in the Eddington approximation (AW; Nobili, Turolla, & Zampieri 1993, hereafter NTZ)

$$\frac{dP}{dy} = \frac{GM_*}{y_G^2 R_*^2}\left(1 - \frac{\kappa_1}{\kappa_{\rm es}}\frac{y_G L}{L_{\rm Edd}}\right), \tag{2}$$

$$\frac{W}{c} = \kappa_P\left(aT^4 - \frac{\kappa_0}{\kappa_P}U\right) + 4\kappa_{\rm es}U\frac{KT}{m_e c^2}\left(1 - \frac{T_\gamma}{T}\right) - \frac{c\kappa_{\rm es}}{8\pi m_e}\int\left(\frac{U_\nu}{\nu}\right)^2 d\nu\,, \tag{3}$$

$$\frac{F_\nu}{cU_\nu}\left[\frac{\partial \ln F_\nu}{\partial y} - \frac{GM_*}{c^2\varrho y_G^2 R_*^2}\left(1 - \frac{\partial \ln F_\nu}{\partial \ln \nu}\right) - \frac{2}{\varrho R_*}\right] = -\frac{s_\nu^0}{y_G U_\nu \varrho}\,, \tag{4}$$

$$\frac{1}{3}\frac{\partial \ln U_\nu}{\partial y} - \frac{GM_*}{c^2\varrho y_G^2 R_*^2}\left(1 - \frac{1}{3}\frac{\partial \ln U_\nu}{\partial \ln \nu}\right) = -\frac{s_\nu^1}{y_G U_\nu \varrho}\,. \tag{5}$$

Here $U = \int U_\nu d\nu$, $L = 4\pi R_*^2 \int F_\nu d\nu$, $L_{\rm Edd} = 4\pi GM_* c/\kappa_{\rm es}$; $\kappa_{\rm es}$, κ_P, κ_0, and κ_1 are the scattering, Planck, absorption, and flux mean opacities, and the radiation temperature T_γ is defined by

$$T_\gamma = \frac{h}{4k}\frac{\int \nu U_\nu d\nu}{\int U_\nu d\nu}\,. \tag{6}$$

$W = W_h - W_c$ represents that part of the injected heat, W_h, which is effectively converted into electromagnetic radiation within the atmosphere. W_c mimics the possible presence of other forms of energy transport (like convection and electron conduction) which are not treated in detail here (see AW for comparison); the actual form of W_c is discussed later on. The first two moments of the source function, s_ν^0 and s_ν^1, account for the exchange of energy and momentum between electrons and photons and, for the radiative processes we are considering, bremsstrahlung and electron scattering, they have the form (NTZ)

$$\frac{s_\nu^0}{U_\nu} = \kappa_{\rm es}\varrho\left\{\frac{kT}{m_e c^2}\left[\frac{\partial^2 \ln U_\nu}{\partial \ln \nu^2} + \left(\frac{\partial \ln U_\nu}{\partial \ln \nu} + \frac{h\nu}{kT} - 3\right)\frac{\partial \ln U_\nu}{\partial \ln \nu} + \frac{h\nu}{kT} + \frac{c^3 U_\nu}{4\pi kT\nu^2}\left(\frac{\partial \ln U_\nu}{\partial \ln \nu} - 1\right)\right] + \frac{\kappa_{\rm ff}}{\kappa_{\rm es}}\left[\frac{4\pi B_\nu(T)}{U_\nu c} - 1\right]\right\} \tag{7}$$

$$s_\nu^1 = -(\kappa_{\rm es} + \kappa_{\rm ff})\varrho\frac{F_\nu}{c}\,, \tag{8}$$

where $B_\nu(T)$ is the Planck function. The free-free opacity for a completely ionized hydrogen gas is

$$\kappa_{\rm ff} = 1.318 \times 10^{56}\varrho T^{-1/2}\frac{1 - e^{-h\nu/kT}}{\nu^3}\bar{g}(\nu, T)\ {\rm cm^2\ g^{-1}}\,,$$

and a functional fit to Karzas & Latter's (1961) tables was used for the velocity-averaged Gaunt factor. Since equations (4) and (5) define a second-order elliptic operator, conditions must be described on the entire boundary of the integration domain and their form is discussed in NTZ. In particular, we assume that diffusion holds in the deeper layers where LTE is certainly attained and this automatically fixes the luminosity at the inner boundary, $L_{\rm in}$. If all the energy is supplied by accretion, the total radiative flux that crosses the inner boundary must equal the heat transported inward by nonradiative processes, that is to say,

$$W_c = \frac{L_{\rm in}}{8\pi R_*^2 y_0 y_G}\frac{1 + v_{\rm th}^2/v_i^2}{[1 - (1 - v_{\rm th}^4/v_i^4)(y/y_0)]^{1/2}}\,, \qquad 0 \le y \le y_{\rm in}\,.$$

Although the total radiation energy density and luminosity are just the integrals of U_ν and $4\pi R_*^2 F_\nu$ over frequency, we found it numerically more convenient to derive them from the first two gray moment equations

$$\frac{dL}{dy} = -\frac{4\pi R_*^2 W}{y_G}\,, \tag{9}$$

$$\frac{1}{3}\frac{dU}{dy} = \kappa_1\frac{L}{4\pi R_*^2 c y_G}\,. \tag{10}$$

Equation (9) gives trivially

$$L = \begin{cases} \dfrac{L_\infty}{y_G^2} - \left(\dfrac{L_\infty}{y_G^2} - L_{\rm in}\right) \dfrac{1 - [1 - (1 - v_{\rm th}^4/v_i^4)(y/y_0)]^{1/2}}{1 - v_{\rm th}^2/v_i^2} & y \le y_0 , \\ L_{\rm in} & y > y_0 , \end{cases} \tag{11}$$

with the condition $L(y_{\rm in}) = L_{\rm in}$, while equation (10) is integrated numerically along with the system (2)–(5), imposing $U(0) = 2F(0)/c$; pressure vanishes at the top of the atmosphere, $P(0) = 0$.

3. RESULTS

Equations (2)–(5) and (10) were solved numerically by means of a finite differences relaxation scheme (NTZ) on a logarithmic grid of 50 frequency bins × 100 depth zones. The adimensional frequency $x = h\nu/kT_*$ was used, $T_* = T(y_{\rm in})$, and the integration range was typically $-0.7 < \log x < 1.1$, $-7.6 < \log y < \log y_{\rm in}$ with $y_{\rm in}$ marginally smaller than y_0. A typical run required ~15 minutes of CPU time on an IBM RISC/6000. Two sets of models were computed, both with $R_* = 12.4$ km, $M_* = 1.4\,M_\odot$: $y_0 = 20$ g cm^{-2} and luminosities in the range $10^{-7} \le L_\infty/L_{\rm Edd} \le 0.2$, $y_0 = 5$ g cm^{-2} and $10^{-7} \le L_\infty/L_{\rm Edd} \le 10^{-5}$. Our numerical method should guarantee a fractional accuracy better than 1% on all the variables. As a further check, the total luminosity, given by equation (11), was compared with the numerical integral of F_ν over the frequency mesh at each depth: agreement was always better than 10%. We have also verified that our solutions with $L_\infty \gtrsim 10^{-2}\ L_{\rm Edd}$ reproduce almost exactly those computed by AW. For low-luminosity models, which we are mainly interested in, particular care must be used to handle properly the absorption and flux mean opacities, since the envelope thermal balance depends entirely on the free-free integrated source term and the radiation spectrum becomes very nearly Planckian in the deeper layers.

Results are summarized in Figures 1, 2, and 3. where the emergent spectra and the temperature profiles are plotted for different values of L_∞. In all these models it is $y_0 = 20$ g cm^{-2}; solutions with $y_0 = 5$ g cm^{-2} show the same qualitative behavior. A quite unexpected feature emerging from Figures 1 and 2 is that the spectral shape deviates more and more from a blackbody as L_∞ decreases. The model with $L_\infty = 2.25 \times 10^{-2} L_{\rm Edd}$ is, in fact, quite Planckian in shape (see also AW), showing only a moderate hard excess. On the contrary, solutions with $L_\infty < 10^{-4} L_{\rm Edd}$ are characterized by a very broad maximum and by a slow decay at high energies. Comptonization is relatively important for $L \gtrsim 10^{-2} L_{\rm Edd}$, similarly to what happens in X-ray burster atmospheres (see, e.g., London, Taam, & Howard 1986). For less luminous models, however, nonconservative scatterings play essentially no role in the formation of the spectrum, as it should be expected since the temperature, and hence the Compton parameter, becomes lower. As can be seen from Figure 3, the temperature profile is nearly adiabatic in the inner layers where the gas is optically thick to true emission-absorption at all frequencies; for $L \lesssim 10^{-5} L_{\rm Edd}$ an intermediate, isothermal region is present. The sudden increase of T in the external layers is due to the heating produced by the incoming protons, balanced mainly by Compton cooling at low densities. The temperature "shock" moves at very low values of the column density and is nearly out of our depth mesh for $L_\infty = 10^{-7} L_{\rm Edd}$.

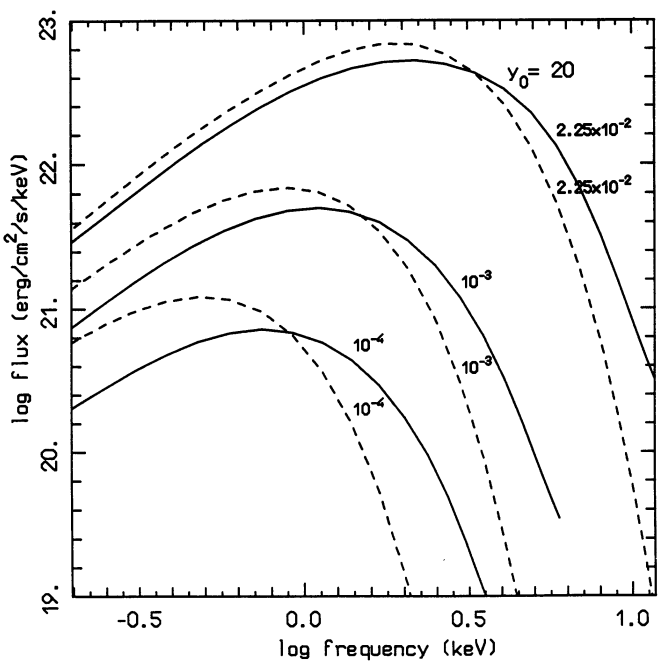

FIG. 1

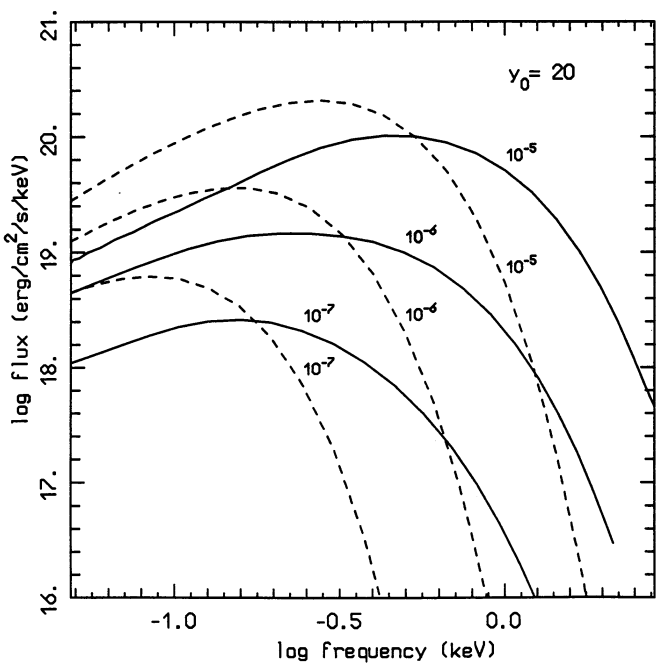

FIG. 2

FIG. 1.—Emergent spectra for $L_\infty = 2.25 \times 10^{-2}$, 10^{-3}, $10^{-4} L_{\rm Edd}$ (*solid lines*), together with the corresponding blackbody spectra at the neutron star effective temperature (*dashed lines*).

FIG. 2.—Same as in Fig. 1 for models with $L_\infty = 10^{-5}, 10^{-6}, 10^{-7} L_{\rm Edd}$

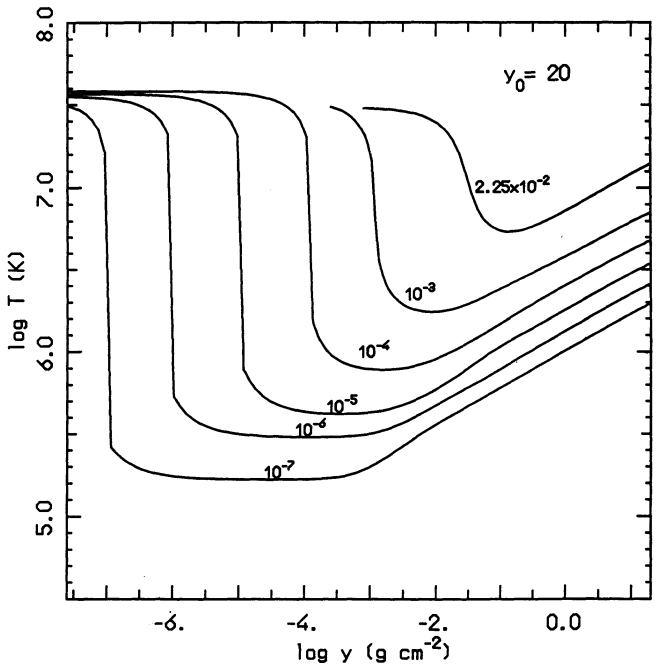

FIG. 3.—Temperature vs. column density for different values of $L_\infty/L_{\rm Edd}$

Although the hard excess present in our low-luminosity spectra may be of interest as far as predictions on the observability of ONSs are concerned, more important, in this respect, seems to be the comparison of the actual emerging spectrum with the blackbody at the neutron star effective temperature, $B_\nu(T_{\rm eff})$, $T_{\rm eff} = [L_\infty/(4\pi R_*^2\,\sigma)]^{1/4}$, which was assumed to be the emitted spectrum in all previous investigations (e.g., Treves & Colpi 1991; Blaes & Madau 1993). It is apparent from Figure 2 that model spectra with $L \lesssim 10^{-5} L_{\rm Edd}$ are substantially harder than the blackbody at the star effective temperature. The spectral hardening can be quantified introducing a hardening ratio

$$\gamma = \frac{T_\gamma}{T_\gamma[B_\nu(T_{\rm eff})]}\,, \tag{12}$$

where the radiation temperature T_γ is defined in equation (6) and $T_\gamma[B_\nu(T_{\rm eff})] = 0.96 T_{\rm eff}$. This differs from the usual definition, $\gamma = T_{\rm col}/T_{\rm eff}$, where $T_{\rm col}$ is the color temperature, because our spectra are not always well fitted by a blackbody. For $y_0 = 20$ g cm^{-2}, γ steadily increases from ~ 1.5 (value typical of X-ray bursters in the static phase), for $L \sim 10^{-2}$–$10^{-3} L_{\rm Edd}$, up to ~ 2.5 for $L \sim 10^{-6}$–$10^{-7} L_{\rm Edd}$ (see Table 1).

4. DISCUSSIONS AND CONCLUSIONS

The significant deviation of low-luminosity spectra from a Planckian equilibrium distribution could appear unexpected, since radiation is in LTE in a medium where the scattering depth is always much less than the absorption one. The source function should be Planckian and the emergent spectrum, formed at the thermal photosphere, should coincide with $B_\nu(T_{\rm eff})$. However, if the atmosphere develops smooth temperature and density gradients in layers where the medium becomes optically thin to free-free, the

TABLE 1

CHARACTERISTIC PARAMETERS FOR SELECTED MODELS

$L_\infty/L_{\rm Edd}$	T_γ (keV)	$F_{>0.1}{}^{a}/F^{\rm bb}_{>0.1}$	γ^{b}	γ^{c}
2.25×10^{-2}.....	1.03	1.01	1.40	...
10^{-3}.....	0.53	1.03	1.56	...
10^{-4}.....	0.35	1.01	1.88	...
10^{-5}.....	0.24	1.02	2.21	2.06
10^{-6}.....	0.15	1.07	2.44	2.31
10^{-7}.....	0.09	1.34	2.64	2.55

[a] Ratio of integrated flux to blackbody one above 0.1 keV, for models with $y_0 = 20$ g cm^{-2}.

[b] Hardening ratio, defined in eq. (12), for models with $y_0 = 20$ g cm^{-2}.

[c] Hardening ratio for models with $y_0 = 5$ g cm^{-2}.

differential nature of absorption opacity plays an important role. High-frequency photons decouple in the deeper, hotter layers and then propagate freely to infinity, contributing to the high-energy part of the emergent spectral flux. At large enough frequencies, the observed shape of the spectrum turns out to be a superposition of Planckians at different temperatures. This result resembles closely that of standard accretion disks, where the emergent spectrum shows a broad plateau due to the combined, thermal emission of rings at different temperatures.

Our present result that low-luminosity spectra are harder than a blackbody is consistent with the previous finding by Romani (1987), who computed model atmospheres for cooling neutron stars. Although he considered a quite different physical scenario, an atmosphere in radiative energy equilibrium illuminated from below, the free-free opacity in his cool, He models ($T_{\rm eff} \sim 3 \times 10^5$ K) acts much in the same way as in our faint solutions, producing a hardening of the spectrum. Both in Romani's and in our analysis the effects of the neutron star magnetic field were ignored. An insight on the role of a strong $\boldsymbol{B}$ field, $\sim 10^{12}$ G, on radiative transfer was recently provided by Miller (1992), who showed that departures from a blackbody become less pronounced, since opacity is increased by magnetic effects. Finally we note that the assumption of a pure hydrogen chemical composition used here, is not entirely ad hoc. In fact, contrary to what happens in equilibrium atmospheres, such as those considered by Romani and Miller who allowed for different compositions, it is likely that metals are destroyed in the accretion flow (Bildsten et al. 1992), leaving just a hydrogen envelope.

As we already stressed, a motivation for studying the spectral properties of X-ray radiation coming from neutron stars accreting at low rates, stems from the possible detection of isolated objects fed by the interstellar gas. Their expected luminosities, $\sim 10^{31}$ ergs s^{-1}, could be within reach of satellites like *Einstein* and *ROSAT* (see Treves & Colpi 1991; Blaes, & Madau 1993; Colpi, Campana, & Treves 1993; Madau, & Blaes 1994). Very recently Stocke et al. (1994) pointed out that one of the objects in the *Einstein* Extended Sensitivity Survey may be actually an ONS, consistently with the original suggestion by Treves & Colpi. The knowledge of the emitted spectrum is fundamental in estimating the observability of any X-ray source and a detailed analysis of the consequences of our results on the detectability of ONSs with *ROSAT* will be presented in forthcoming paper (Colpi et al. 1995). Here we point out that synthetic spectra, being significantly harder than the blackbody at $T_{\rm eff}$, may indeed increase the chances of detection. In Table 1 we have listed the ratios of the computed flux above 0.1 keV to the blackbody one for various luminosities; the threshold of 0.1 keV was suggested by the sensitivity of *ROSAT*. The solutions with $L = 10^{-7}$ and $10^{-5} L_{\rm Edd}$ can be taken as representative of the typical luminosities expected from ONSs embedded in the average ISM or in Giant Molecular Clouds (see Colpi et al. 1993). As can be seen from Table 1, the ratio becomes larger than unity and the flux above 0.1 keV is from $\sim 10\%$ to $\sim 40\%$ larger than the blackbody one for $10^{32} \gtrsim L \gtrsim 10^{31}$ ergs s^{-1}.

Our present models could be relevant also to Soft X-ray Transients in quiescence, such as Aql X-1 (Verbunt et al. 1994), or in connection with low-luminosity globular cluster X-ray sources which emit a luminosity $\sim 10^{-4} L_{\rm Edd}$ (see, e.g., Hertz, Grindlay, & Bailyn 1993 and references therein). These still mysterious objects could be either accreting white dwarfs (e.g., cataclysmic variables) or neutron stars in binary systems. Their spectrum, which is still poorly known, could be compared with the results of our model, and deviations from a blackbody could be an important clue in discriminating their physical nature.

We thank an anonymous referee for some helpful comments.

REFERENCES

Alme, M. L., & Wilson, J. R. 1973, ApJ, 186, 1015 (AW)
Bildsten, L., Salpeter, E. E., & Wasserman, I. 1992, ApJ, 384, 143
Blaes, O., & Madau, P. 1993, ApJ, 403, 690
Colpi, M., Campana, S., & Treves, A. 1993, A&A, 278, 161
Colpi, M., Treves, A., Turolla, R., Zampieri, L., & Zane, S. 1995, in preparation
Hertz, P., Grindlay, J. E., & Bailyn, C. D. 1993, ApJ, 410, L87
Karzas, W. J., & Latter, R. 1961, ApJS, 6, 167
London, R. A., Taam, R. E., & Howard, W. E. 1986, ApJ, 306, 170
Madau, P., & Blaes, O. 1994, ApJ, 423, 748
Miller, M. C. 1992, MNRAS, 255, 129
Nobili, L., Turolla, R., & Zampieri, L. 1993, ApJ, 404, 686 (NTZ)
Ostriker, J. P., Rees, M. J., & Silk, J. 1970, Astrophys. Lett., 6, 179
Romani, R. W. 1987, ApJ, 313, 718
Shapiro, S. L., & Salpeter, E. E. 1973, ApJ, 198, 761
Stocke, J. T., Wang, Q. D., Perlman, E. S., Donahue, M., & Schachter, J. 1994, preprint
Treves, A., & Colpi, M. 1991, A&A, 241, 107
Turolla, R., Zampieri, L., Colpi, M., & Treves, A. 1994, ApJ, 426, L35 (Paper I)
Verbunt, F., Belloni, T., Johnston, H. M., Van der Klis, M., & Lewin, W. H. G. 1994, A&A, 285, 903
Zel'dovich, Ya., & Shakura, N. 1969, Soviet Astron.—AJ, 13, 175, (ZS)